

Nonlinear and crack propagation analysis of concrete dams: A comparative study of 2D and 3D models

Nghia Trong Nguyen^{1*}, My Ngoc Tra Lam², Hung Sy Nguyen²

¹Ho Chi Minh City Open University, Ho Chi Minh City, Vietnam

²Ho Chi Minh City University of Technology and Education, Ho Chi Minh City, Vietnam

*Corresponding author: nghia.nt@ou.edu.vn

ARTICLE INFO

DOI:10.46223/HCMCOUJS.
acs.en.14.2.58.2024

Received: June 03rd, 2024

Revised: June 24th, 2024

Accepted: July 10th, 2024

Keywords:

2D analysis; 3D analysis;
concrete gravity dam; crack
propagation; dynamic analysis;
plastic damage

ABSTRACT

The nonlinear behavior and crack propagation in concrete dams, particularly at spillway sections where section variations can induce excessive local stresses, pose significant challenges for designers. While many designs rely on 2D models due to their simplicity and reduced computational demands, this common approach may underestimate stress concentrations and potential damage at critical spillway sections. This study undertakes a comparative analysis of 2D and 3D simulations of a concrete gravity dam using the finite element program ABAQUS. Our findings indicate that 3D simulations more accurately detect damage at stress concentration points, underscoring the importance of employing rigorous 3D models for complex sections of concrete gravity dams to ensure structural integrity and safety.

1. Introduction

Concrete dams are massive structures that can significantly impact local communities and have national implications. Ensuring the safety of these dams is paramount during both design and construction phases. Rigorous analysis, particularly of concrete damage during strong earthquakes, is essential for informed decision-making by various levels of management and investment stakeholders. Numerous researchers have investigated the damage to concrete gravity dams through various approaches. For instance, Zhang, Wang, and Sa (2013) simulated seismic sequences to evaluate the damage to concrete gravity dams, while Zhang and Wang (2013) examined the effects of fault proximity on dam damage. Alembagheri and Ghaemian (2013a) used capacity estimation approaches to assess dam damage, and in another study (Alembagheri & Ghaemian, 2013b), they evaluated a concrete arch dam using nonlinear incremental dynamic analysis. Calayir and Karaton (2005) employed a continuum damage concrete model for earthquake analysis of dam-reservoir systems. These assessments are vital; however, the common design approach relies on 2D simulations due to their simplicity and computational efficiency. Such simplifications can lead to significant issues, especially in complex sections like spillways. Therefore, it is crucial to accurately evaluate these sections and compare the effects of 2D and 3D simulations to ensure comprehensive safety assessments.

In this study, we conducted a rigorous analysis of 2D and 3D simulations of spillway sections, incorporating the concrete damage plasticity model under seismic impact. The applied strong ground motion, derived from previous research on the Koyna Dam, corresponded to a 6.5 Richter scale earthquake, which significantly affected the Koyna Dam's structure. Crack propagation was meticulously monitored during seismic events, revealing that the dam neck was

the weakest zone, where cracks first appeared. The 3D simulation showed more severe crack patterns compared to the 2D simulation, highlighting that section variations cause significant localized stress, which in turn influences the crack distribution in concrete gravity dams.

2. Modelling

The proposed geometry for the spillway section features a height of 117 meters with a water level of approximately 106 meters, as shown in Figure 1. The base section has been enlarged to 99.1 meters, while the top section measures 26.6 meters. Based on this geometry, 2D and 3D simulation models were developed, as illustrated in Figure 2. The 2D meshing model comprises 486 elements (4-node elements), whereas the 3D meshing model consists of 8,214 elements (8-node solid elements). While the computational time for the 3D model is anticipated to be higher than that for the 2D model, the 3D model provides a geometry that more accurately represents the real structure.

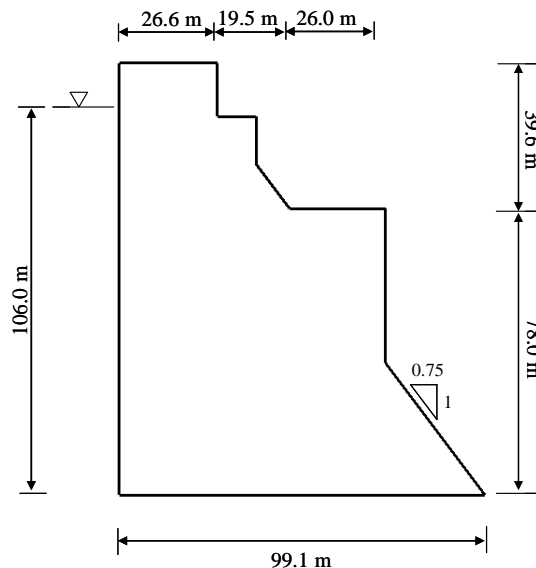


Figure 1. Geometry

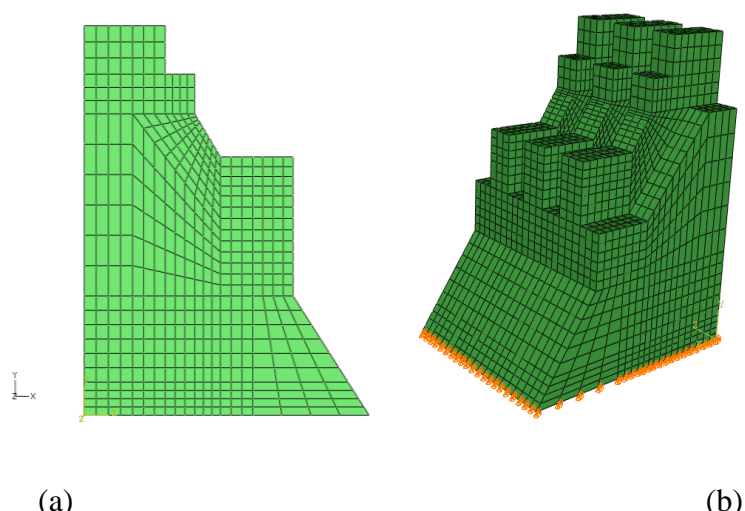


Figure 2. Meshes: (a) 2D model; (b) 3D model

Seismic analysis of concrete dams typically involves considering the interactions between the dam, the water it holds, and its foundation, along with a detailed cracking model. This study aims to investigate the behavior of a concrete gravity dam subjected to strong ground motion, employing certain simplifying assumptions to streamline the analysis. Specifically, a full-scale concrete gravity dam is modeled under the assumption of a rigid foundation, thereby neglecting dam-foundation interactions. To account for the dynamic interactions between the dam and the reservoir, the Westergaard added mass technique is utilized. This method incorporates hydrodynamic forces by adding equivalent mass to the structure, thus approximating the impact of water on the dam during seismic events.

The general equation of motion for a concrete gravity dam subjected to strong ground motion is:

$$[M]\ddot{\{u\}} + [C]\dot{\{u\}} + [K(t)]\{u\} = \{F(t)\} \quad (1)$$

Where

$[M]$ is the mass matrix including added mass for impounded water; $[C]$ is the damping matrix; $[K(t)]$ is the stiffness matrix at time t . In non-linear analysis, the stiffness of construction changes with time; $\ddot{\{u\}}$ is acceleration vector; $\dot{\{u\}}$ is the velocity vector; $\{u\}$ is displacement vector; $\{F(t)\}$ is external force vector, that is the combination of the static load vector and the earthquake load vector.

The impact of hydrodynamic forces was simplified in this study using the added-mass technique proposed by Westergaard (1933). This method approximates the hydrodynamic stresses exerted by the water behind the gravity dam by distributing these stresses in direct relation to ground motion. The calculated stresses were integrated back into the model through a user-defined element code (UEL) provided by ABAQUS, ensuring a more accurate simulation of the hydrodynamic effects on the dam structure.

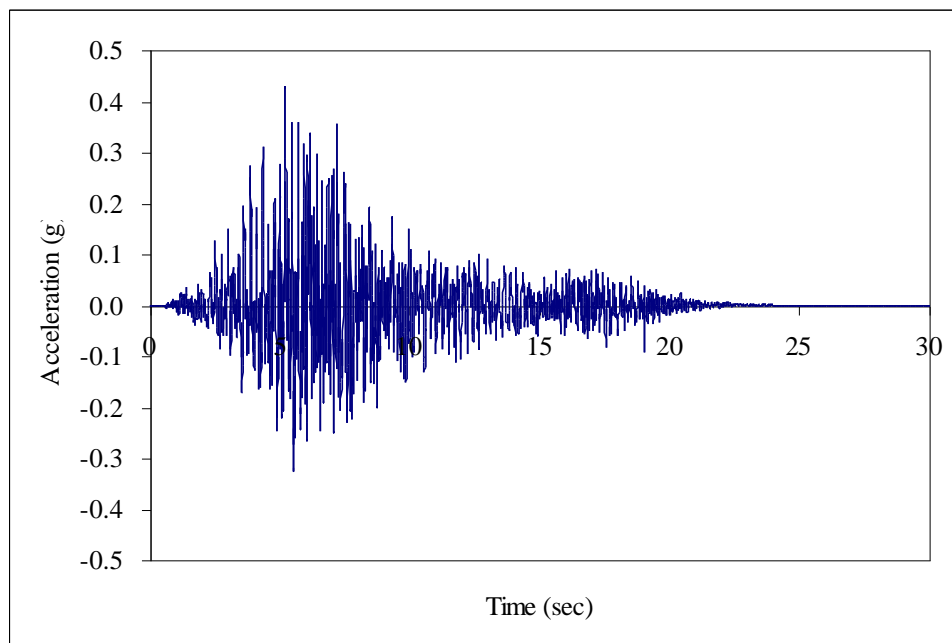
Additionally, the impact of base stiffness was simplified in this study by assuming that the dam base was fixed, based on the assumption that the dam is situated on a stiff rock. Ground motions were applied at the dam base, using the same ground motion data recorded at the Koyna Dam in India in 1967. As illustrated in Figure 3, the ground motion reached its peak acceleration of approximately 0.4g at around 05 seconds before gradually decaying over the subsequent 25 seconds. This ground motion is enough to cause serious damage to the structure of the Koyna dam (Chopra & Chakrabarti, 1973). The concrete material used was proposed with several typical parameters illustrated in Table 1.

The simulation procedure involved several key steps, beginning with a frequency analysis to determine the damping factor, followed by a dynamic analysis to assess crack propagation. By comparing the results from both the 2D and 3D simulations, we were able to thoroughly investigate the differences and impacts of each simulation approach.

Table 1

Concrete parameters

| Parameters | Unit | Value |
|----------------------|-------------------|-------|
| Unit weight | g/cm ³ | 2,400 |
| Elastic modulus | GPa | 30 |
| Poisson's ratio | None | 0.2 |
| Dilation angle | Degree | 36.3 |
| Tensile strength | MPa | 2.5 |
| Compressive strength | MPa | 15 |

**Figure 3.** Ground motion

In ABAQUS, the mechanical behavior of concrete can be formulated by the plastic-damage constitutive model (Lee & Fenves, 1998; Lubliner, Oliver, Oller, & Oñate, 1989). Based on the non-associative flow rule, the plastic potential function and the yield function are given in stress space as follows.

(1) Plastic potential function:

The flow potential function, based on the modified Drucker-Prager hyperbolic function, is given by:

$$G = \sqrt{(\varepsilon\sigma_{t0} \tan \Psi)^2 + \bar{q}^2} - \bar{p} \tan \Psi \quad (2)$$

With

$$\bar{p} = -\frac{1}{3} \text{trace}(\bar{\sigma}) \quad (3)$$

$$\bar{q} = \sqrt{\frac{3}{2}(\bar{S} : \bar{S})} \quad (4)$$

$$\bar{S} = \bar{\sigma} + \bar{p}I \quad (5)$$

Where \bar{S} is the effective stress deviator, $\Psi(\theta, f_i)$ is the dilation angle measured in the p-q plane at high confining pressure, $\sigma_{t0}(\theta, f_i) = \sigma_t / \varepsilon_t^{pl} = 0, \varepsilon_t^{pl} = 0$ is the uniaxial tensile stress at failure, taken from the user-specified tension stiffening data and $\varepsilon(\theta, f_i)$ is a parameter that defines the rate at which the function approaches the asymptote.

(2) Yield function

The yield function formulated in stress space is given by

$$F = \frac{1}{1-\alpha} \left(\bar{q} - 3\alpha\bar{p} + \beta(\tilde{\varepsilon}^{pl}) \left\langle \hat{\bar{\sigma}}_{\max} \right\rangle - \gamma \left\langle -\hat{\bar{\sigma}}_{\max} \right\rangle \right) - \bar{\sigma}_c(\tilde{\varepsilon}_c^{pl}) = 0 \quad (6)$$

$$\text{Where } \alpha = \frac{(\sigma_{b0}/\sigma_{c0}) - 1}{2(\sigma_{b0}/\sigma_{c0}) - 1}; 0 \leq \alpha \leq 0.5, \quad \beta = \frac{\bar{\sigma}_c(\tilde{\varepsilon}_c^{pl})}{\bar{\sigma}_t(\tilde{\varepsilon}_t^{pl})} (1-\alpha) - (1+\alpha) \text{ and } \gamma = \frac{3(1-K_c)}{2K_c - 1}$$

$\hat{\bar{\sigma}}_{\max}$ is the maximum principal effective stress, σ_{b0}/σ_{c0} is the ratio of initial biaxial compressive yield stress to initial uniaxial compressive yield stress, and K_c is the ratio of the second stress invariant on the tensile meridian to the compressive meridian at initial yield for any given value of the pressure invariant p .

3. Results and discussion

Based on the results of the frequency simulations, there were slight differences in the first mode frequencies, with the 2D simulation yielding 2.7Hz and the 3D simulation yielding 2.87Hz. These minor variations suggest that the dynamic responses of the 2D and 3D models are comparable, indicating that the 2D model can, to some extent, represent the real structure. The damping parameters were determined as a function of the first mode frequency using the following relationship:

$$\beta = 2\xi_1/\omega_1 \quad (7)$$

Where ω_1 is the frequency of the first model, and 1 is a fraction of critical damping.

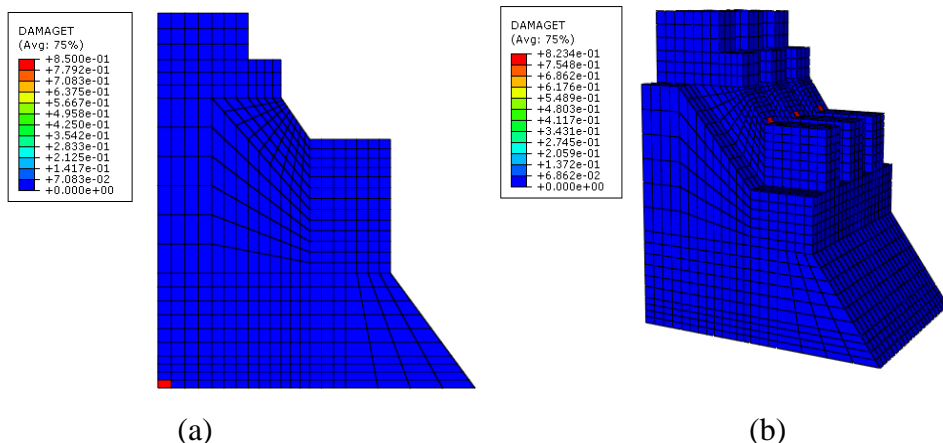


Figure 4. The initial damage location;

(a) 2D simulation at 5.040 seconds; (b) 3D simulation at 3.952 seconds

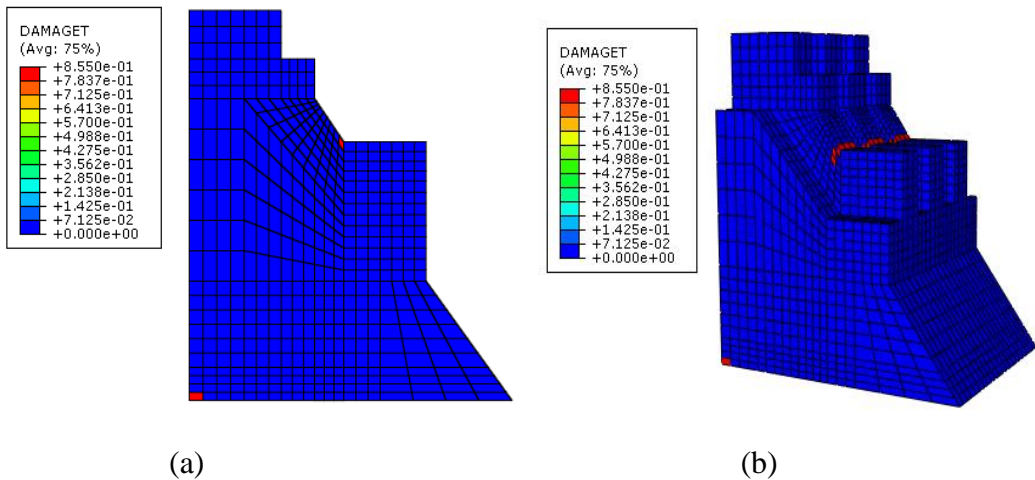


Figure 5. The second damage location;
(a) 2D simulation at 5.840 seconds; (b) 3D simulation at 4.067 seconds

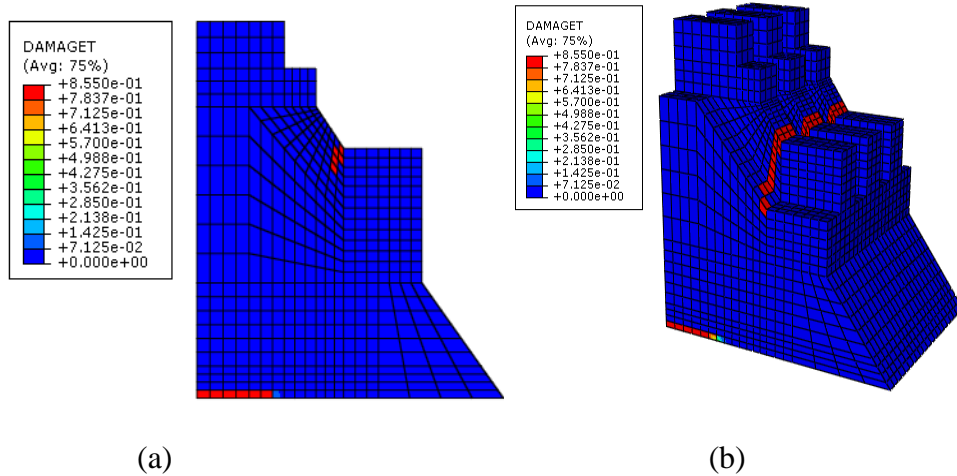


Figure 6. The final damage; (a) 2D simulation; (b) 3D simulation

Table 2

Summary of comparison 2D and 3D analysis

| Case | Relative Time points | Time (sec) | Acceleration (g) |
|------|----------------------|------------|------------------|
| 2D | 1 st dam. | 5.040 | 0.07225 |
| | 2 nd dam. | 5.840 | 0.16023 |
| | Max dam. | 7.757 | 0.08715 |
| 3D | 1 st dam. | 3.952 | 0.00381 |
| | 2 nd dam. | 4.067 | -0.0497 |
| | Max dam. | 6.25 | -0.1866 |

Dynamic analysis revealed differences in the first damage locations between the 2D and 3D simulations, as shown in Figure 4 and summarized in Table 2. In the 2D simulation, the first damage appeared at the dam's base at 5.040 seconds, whereas in the 3D simulation, the initial damage occurred at the dam's neck at 3.952 seconds. This indicates that at the time when the 3D model shows initial damage, the 2D model does not yet exhibit any damage. Additionally, the

3D model's identification of the dam neck as the critical zone where the initial crack propagation occurs, highlights the impact of localized stress in this area. This stress localization, captured by the 3D model, underscores the importance of using more comprehensive simulations to accurately identify potential weak points in the structure.

Similarly, the second damage locations for both 2D and 3D simulations, as shown in Figure 5, were observed at the dam's base and neck. Interestingly, in the 3D simulation, the second damage location emerged at 4.067 seconds, which is even earlier than the first damage location in the 2D simulation at 5.040 seconds. This clearly indicates that the 2D simulation misses the critical times where overstress and damage occur. This discrepancy is likely due to the localized stress concentrations, as previously mentioned, which the 3D simulation effectively captures. These findings underscore the importance of using 3D simulations to accurately predict and analyze the behavior of concrete dams under seismic loading, particularly in identifying critical damage points that may be overlooked in simpler 2D models.

The final damage observed in both 2D and 3D simulations is depicted in Figure 6, with the 3D simulations revealing more extensive damage, particularly at the dam's neck. This outcome is expected due to the geometric variations that 3D simulations can more accurately capture. Despite its simplifications, the 2D model also correctly identified the two weak locations, though the crack patterns were less pronounced compared to the 3D results. This study provides a comprehensive understanding of how geometry affects crack propagation and highlights the impact of using 2D versus 3D simulations on estimating crack patterns. The earlier crack propagation in the 3D simulation compared to the 2D simulation can be attributed to stress localization. This research offers valuable insights into the effects of different simulation approaches, aiding designers and managers in understanding crack propagation dynamics and making informed engineering decisions.

4. Conclusions & recommendations

This study compared 2D and 3D simulation approaches. Key findings include:

1. The frequency simulations revealed minor differences in the first mode frequencies, with the 2D model at 2.7Hz and the 3D model at 2.87Hz. These slight variations suggest comparable dynamic responses, indicating that the 2D model can, to some extent, represent the real structure's dynamic behavior.
2. The dynamic analysis showed significant differences in the initial damage locations between the 2D and 3D models. The 2D simulation indicated the first damage at the dam's base at 5.04 seconds, while the 3D simulation revealed initial damage at the dam's neck at 3.95 seconds. This discrepancy highlights that the 2D model did not capture early damage observed in the 3D model, emphasizing the impact of localized stress.
3. The 3D model effectively identified the dam neck as a critical zone for initial crack propagation, underscoring the importance of using comprehensive simulations to detect potential weak points in the structure.
4. The second damage locations observed in the 3D simulation at 4.07 seconds occurred even earlier than the first damage in the 2D simulation at 5.04 seconds. This indicates that the 2D model missed critical times of overstress and damage, likely due to the stress localization that the 3D model captured.
5. The final damage analysis showed more extensive damage in the 3D simulations, particularly at the dam's neck, due to geometric variations that the 3D model could more

accurately capture. While the 2D model also identified weak locations, the crack patterns were less pronounced compared to the 3D results.

6. The study demonstrated the significant effect of geometry on crack propagation, with the 3D model providing a more realistic representation of the structure.

These findings underscore the necessity of using 3D simulations for accurately predicting and analyzing the behavior of concrete dams under seismic loading. The comprehensive approach of the 3D model ensures better identification of critical damage points that may be overlooked in simpler 2D models. This research offers valuable insights into crack propagation dynamics, aiding designers and managers in making informed engineering decisions to enhance the safety and integrity of concrete gravity dams.

References

Alembagheri, M., & Ghaemian, M. (2013a). Seismic assessment of concrete gravity dams using capacity estimation and damage indexes. *Earthquake Engineering & Structural Dynamics*, 42(1), 123-144.

Alembagheri, M., & Ghaemian, M. (2013b). Damage assessment of a concrete arch dam through nonlinear incremental dynamic analysis. *Soil Dynamics and Earthquake Engineering*, 44, 127-137.

Calayir, Y., & Karaton, M. (2005). A continuum damage concrete model for earthquake analysis of concrete gravity dam-reservoir systems. *Soil Dynamics and Earthquake Engineering*, 25(11), 857-869.

Chopra, A. K., & Chakrabarti, P. (1973). The Koyna earthquake and the damage to Koyna dam. *Bulletin of the Seismological Society of America*, 63(2), 381-397.

Lee, J., & Fenves, G. L. (1998). Plastic-damage model for cyclic loading of concrete structures. *Journal of Engineering Mechanics*, 124(8), 892-900.

Lubliner, J., Oliver, J., Oller, S., & Oñate, E. (1989). A plastic-damage model for concrete. *International Journal of Solids and Structures*, 25(3), 299-326.

Westergaard, H. M. (1933). Water pressures on dams during earthquakes. *Transactions of ASCE*, 98(2), 418-433.

Zhang, S., & Wang, G. (2013). Effects of near-fault and far-fault ground motions on nonlinear dynamic response and seismic damage of concrete gravity dams. *Soil Dynamics and Earthquake Engineering*, 53, 217-229.

Zhang, S., Wang, G., & Sa, W. (2013). Damage evaluation of concrete gravity dams under mainshock-aftershock seismic sequences. *Soil Dynamics and Earthquake Engineering*, 50, 16-27.

